Eur. Phys. J. B **59**, 527–533 (2007)
DOI: 10.1140/epjb/e2007-00306-1

THE EUROPEAN PHYSICAL JOURNAL B

Maximum entropy principle and coherent harmonic generation using a single-pass free-electron laser

F. Curbis[1,2], A. Antoniazzi[3], G. De Ninno[1,a], and D. Fanelli[3]

[1] Sincrotrone Trieste, S.S. 14 km 163.5, Basovizza, 34012 Trieste, Italy
[2] Università di Trieste, Dipartimento di Fisica, via A. Valerio 2, 34127 Trieste, Italy
[3] Università di Firenze, INFM and INFN, Dipartimento di Energetica, via S. Marta 3, 50139 Firenze, Italy

Received 22 January 2007 / Received in final form 21 August 2008
Published online 15 November 2007 –

Abstract. Single-pass free-electron lasers constitute an example of systems with long-range interactions. The light-particle interplay leading to the power growth and successive relaxation towards a quasi-stationary state is governed by the Vlasov equation. A maximum entropy principle inspired to Lynden-Bell's theory of "violent relaxation" for the Vlasov equation can be invoked to analytically characterize the behaviour of the saturated system. In particular, we here concentrate on the case of coherent harmonic generation obtained from an externally seeded free-electron laser and provide a simple strategy to predict the laser intensity as well as the final electron-beam energy distribution.

PACS. 05.45.-a Nonlinear dynamics and chaos

1 Background

Physical systems are constituted by interacting component elements, e.g. point particles or atoms. In presence of short-range couplings, every element is solely sensitive to the adjacent environment, being therefore uniquely subjected to the interaction with local neighbors. Conversely, when long-range forces are to be considered, a global network of connections is active, each element feeling the direct influence of every other constitutive unit. This crucial distinction is responsible for the enhanced degree of complexity in the treatment of long-range systems when compared to short-range ones. As a consequence, basic concepts in physics, notably in the framework of equilibrium statistical mechanics, have been rigorously developed preferentially with reference to the latter case. The potential interest of such tools is however very broad since for all fundamental interactions in nature (with the exception of gravity), screening mechanisms manifest, resulting in effective short-range couplings. For this reason, until quite recently, it has essentially only been in the context of astrophysics and cosmology that the very specific and difficult features of long-range interactions have been tackled. Recently, however, a growing number of physical laboratory systems have emerged in which the interactions are truly long-range, e.g. unscreened Coulomb interactions, vortices in two-dimensional fluid mechanics, wave-particle systems relevant to plasma physics and Free-Electron Lasers (FEL's). These developments gave new impetus [1] to attempts aiming at describing the peculiar behaviour of long-range interacting systems, in a context where, in contrast to astrophysics, laboratory experiments are possible. Moreover, a number of paradigmatic "toy models" have been proposed that provide the ideal ground for theoretical investigations. Among others, the Hamiltonian Mean Field (HMF) model [2] is nowadays widely analyzed because of its intrinsic simplicity.

Single-pass FEL's are light sources producing powerful (GW) coherent radiation in a wide spectral range (i.e., from infra-red to hard X-rays). They constitute a genuine example of systems with long-range interactions, where the interplay between collective (wave) and individual (particles) degrees of freedom is well known to be central. This interplay being essentially non dissipative, its prototype is described by a self-consistent Hamiltonian [3], which provides a clear and intuitive picture of the basic mechanisms that drive the process of light amplification and saturation. In this respect, FEL's provide a very general experimental ground to investigate the universal features that characterize systems with long range interactions. This includes relaxation to long lived quasi-stationary states (QSS's) before the final thermodynamical equilibrium is reached.

Recently, in [4] and [5] we demonstrated that a maximum entropy principle inspired to Lynden-Bell's theory of "violent relaxation" for the Vlasov equation [6] allows to satisfactorily explain numerical simulations performed for a FEL operated in Self Amplified Spontaneous Emission (SASE) [7] configuration and for the HMF model. A SASE FEL relies on the nonlinear interaction between an un-bunched electron beam and the spontaneous radiation

[a] e-mail: giovanni.deninno@elettra.trieste.it

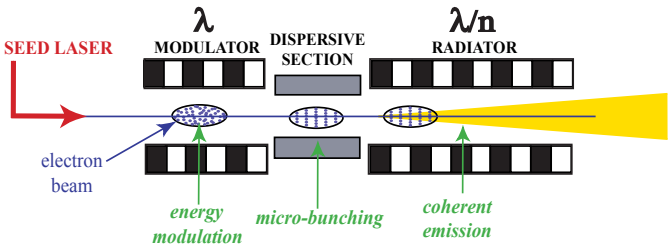

Fig. 1. Schematic layout of the CHG scheme. The electron beam, coming from left, passes through a first undulator, called modulator; the interaction with a synchronized seeding signal (provided, e.g., by a laser) produces a modulation of the electron energy. Then, the beam propagates through a dispersive section, where the energy modulation is converted in spatial modulation (micro-bunching). Finally, in the last undulator, called radiator, the micro-bunched electron beam emits coherently.

it emits when guided by the static and periodic magnetic field generated by an undulator. An alternate configuration to SASE, named in the following Coherent Harmonic Generation (CHG), is the one in which the radiation is produced by electrons pre-bunched by an external source, e.g. a laser field [8]. In this paper we generalize to CHG the results presented in [4] for the restricted case of SASE.

The paper is organized as follows: in Section 2 we introduce the basic concepts on which single-pass FEL's rely (with particular concern to CHG) and we shortly review the self-consistent Hamiltonian formulation [3] that provides a minimalist framework to address the study of the FEL dynamics. Section 3 is devoted to presenting the maximum entropy principle and its application to the case under inspection. Section 4 compares numerical simulations for the CHG FEL to theoretical predictions. Finally, in Section 5 we draw conclusions and outline perspectives.

2 Introduction to the Free Electron Laser physics

In a single-pass FEL, the physical mechanism responsible for the light emission and amplification is the interaction between a relativistic electron beam, a magnetostatic periodic field generated by an undulator and an optical wave co-propagating with electrons. Two different schemes can be distinguished, depending on the origin of the optical wave which is used to initiate the process. In the SASE configuration, the initial seed is provided by the spontaneous emission of the electron beam which is forced by the undulator field to follow a curved trajectory. The seed is then amplified all along the undulator until the laser effect is reached. The SASE radiation produces tunable radiation at short (X-ray) wavelengths with several GW peak power and excellent spatial mode. An alternate approach to SASE is CHG, which is capable of producing temporally coherent pulses. A schematic layout of CHG is shown in Figure 1. In this case, the initial seed is produced by an external light source, e.g. a laser. The light-electron interaction in a short undulator, called modulator, imposes an energy modulation on the electron beam. The modulator is tuned to the seed wavelength λ. The energy modulation is then converted into a spatial density modulation (bunching) as the electron beam transverses a dispersive section, i.e. a region of space where a constant magnetic field induces different paths for electrons having different energies. Figure 2 shows the evolution of the electron-beam phase space (i.e. energy vs. electrons' phase in the undulator plus radiator field) from the entrance of the modulator to the exit of the dispersive section. Finally, in a second undulator, called radiator and tuned at one of the harmonics of the seed frequency, the micro-bunched electron beam emits coherent radiation at the harmonic wavelength.

In the following we introduce the model that can be used to address the study of a single-pass FEL, both in the modulator and radiator of a CHG scheme. By putting forward the hypothesis of one-dimensional (longitudinal) motion, small particle energy spread and monochromatic radiation, the system evolution during the propagation inside each undulator is described by the following set of equations (N being the number of electrons):

$$\frac{\mathrm{d}\theta_j}{\mathrm{d}\bar{z}} = p_j, \tag{1}$$

$$\frac{\mathrm{d}p_j}{\mathrm{d}\bar{z}} = -Ae^{i\theta_j} - A^* e^{-i\theta_j}, \tag{2}$$

$$\frac{\mathrm{d}A}{\mathrm{d}\bar{z}} = \frac{1}{N}\sum_j e^{-i\theta_j}, \tag{3}$$

where $\bar{z} = 2k_u\rho z\gamma_r^2$ is the re-scaled longitudinal coordinate, which plays the role of time. Here, $\rho = (a_w\omega_p/4ck_u)^{2/3}/\gamma_r$ is the so-called Pierce parameter, γ_r the resonant energy, k_u the wave vector of the undulator, $\omega_p = (e^2\bar{n}/m\varepsilon_0)^{1/2}$ the plasma frequency, $\bar{n}$ being the electron number density, c the speed of light, e and m respectively the charge and mass of one electron. Further, $a_w = eB_w/(k_u mc^2)$, where B_w is the rms undulator field. Introducing the wavenumber $k = 2\pi/\lambda$, where λ is the wavelength of the FEL radiation, the phase θ is defined by $\theta = (k + k_u)z - \omega t$, being $\omega = kc$ the radiation frequency; its conjugate momentum reads $p = (\gamma - \langle\gamma_0\rangle)/(\rho\langle\gamma_0\rangle)$, being $\langle\gamma_0\rangle$ the mean energy of the electrons at the undulator's entrance. The complex amplitude $A = A_x + iA_y$ represents the scaled field, transversal to z. We have assume here $\langle\gamma_0\rangle = \gamma_r$ ("perfect tuning" condition). The above system of equations can be deduced from the Hamiltonian

$$H = \sum_{j=1}^{N}\frac{p_j^2}{2} + 2\sqrt{\frac{I}{N}}\sum_{j=1}^{N}\sin(\theta_j - \varphi), \tag{4}$$

where the intensity I and the phase φ of the wave are defined by $A = \sqrt{I/N}\exp(-i\varphi)$. Here the canonically conjugated variables are (p_j, θ_j), for $1 \le j \le N$, and (I, φ). Besides the "energy" H, the total momentum $P = \sum_j p_j + I$ is also a conserved quantity. Let us finally define the bunching parameter for the nth harmonic

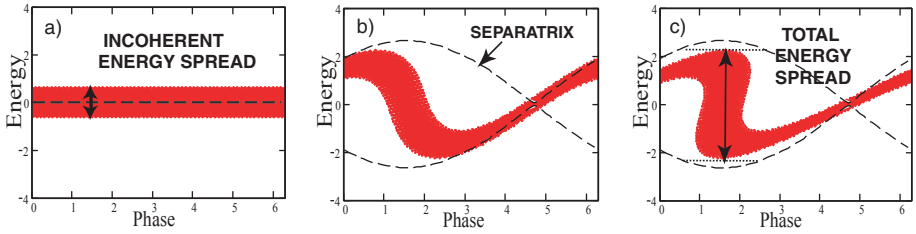

Fig. 2. Electron-beam phase space at the entrance a) and at the exit b) of the modulator; c) phase space at the exit of the dispersive section. In a), the thickness of the distribution corresponds to the (initial) incoherent energy spread of the electron beam. In c) the gap between the boundaries of the separatrix corresponds to the energy modulation induced by the seed-electron interaction (see Fig. 1).

($n = 1, 2, 3, ...$ being an integer number) of the optical wave as $b_n(\bar{z}) = \sum \exp(in\theta_i(\bar{z}))/N := \langle \exp(in\theta(\bar{z})) \rangle$. The latter provides a quantitative measure of the degree of spatial compactness of the particles distribution at the scale of the wavelength λ/n.

More specifically, in the modulator, A represents the (high power) field provided by the external seed. As shown in Figure 2, the seed-electron interaction induces a coherent modulation, $\Delta\gamma$, of the electron-beam energy, which combines to the initial incoherent energy spread σ_γ. At the modulator entrance electrons are randomly distribued in phase and, as a consequence, the initial bunching is virtually zero (not exactly zero, due to granularity). Substantial bunching at the fundamental and higher harmonics is created inside the dispersive section, where energy modulation is converted into spatial density modulation. Indeed, performing a Fourier analysis of the spatial beam distribution at the end of the dispersive section one finds the following harmonic (i.e., bunching) coefficients [9]:

$$|b_n| = |\langle \exp(in\theta) \rangle| = \exp\left[-\frac{1}{2} n^2 \sigma_\gamma^2 d^2\right] J_n\left[nd\Delta\gamma\right], \quad (5)$$

where d is the strength of the dispersive section (that is directly related to the peak value of the static magnetic field) and J_n stands for the nth order Bessel function. Significant bunching is obtained if $d\Delta\gamma \simeq 1$. Conversely, the first exponential factor in the previous equation shows that the incoherent energy spread σ_γ erases the bunching when $n^2\sigma_\gamma^2 d^2 > 1$. Hence, in order to have strong bunching parameter at the nth harmonic, the energy modulation must be at least equal to n times the energy spread: $\Delta\gamma = n\sigma_\gamma$. The total energy spread $\sigma_{\gamma,tot}$ at the entrance of the radiator reads:

$$\sigma_{\gamma,tot} = \sqrt{\sigma_\gamma^2 + \frac{(\Delta\gamma)^2}{2}}. \quad (6)$$

The radiator is tuned at the harmonic λ/n^*. Coherent emission at such wavelength is driven by the corresponding bunching coefficient, defined by equation (5) with $n = n^*$. In other words, equations (5) and (6) define the initial conditions at the radiator entrance.

The above model represents a paradigmatic example of wave-particles interaction, where the direct coupling of each element to every other element belonging to the system has to be accounted for. The system is hence dominated by mean-field effects, which constitute a specific class of long range forces.

Numerical simulations based on system (1-3) show that the amplification of the wave inside the radiator occurs in several subsequent steps, see the curve in Figure 7. First, a quadratic growth takes place. Then, after an exponential regime, the system attains a quasi stationary state, where the wave intensity displays oscillations around a well-defined plateau. As predicted by the Boltzmann-Gibbs statistics, for longer times the system relaxes toward the final (thermodynamical) equilibrium. The process is driven by granularity and the time for the relaxation to occur diverges with the system size N. Hence, due to the constraint imposed by the typical length of an undulator (several meters) and by the very large number of particles (order of 10^{10}), the QSS is the only regime experimentally accessible in the case of single-pass FEL's.

When the system reaches the QSS, a portion of particles cluster in phase-space and give birth to a coherent clump which rotates in the bucket created by the wave, synchronized with the oscillations of the intensity. The remaining particles are uniformly distributed between two oscillating boundaries, as shown in Figure 3 [10,11].

3 Statistical prediction in the Vlasov-Wave framework

The initial growth and relaxation towards the QSS are governed by the Vlasov equation [12], which is obtained by performing the continuum limit, namely $N \to \infty$ at fixed volume and energy per particle, in the system of equations (1-3):

$$\frac{\partial f}{\partial \bar{z}} = -p\frac{\partial f}{\partial \theta} + 2(A_x \cos\theta - A_y \sin\theta)\frac{\partial f}{\partial p}, \quad (7)$$

$$\frac{dA_x}{d\bar{z}} = + \int f \cos\theta \, \mathrm{d}\theta \, \mathrm{d}p, \quad (8)$$

$$\frac{dA_y}{d\bar{z}} = - \int f \sin\theta \, \mathrm{d}\theta \, \mathrm{d}p. \quad (9)$$

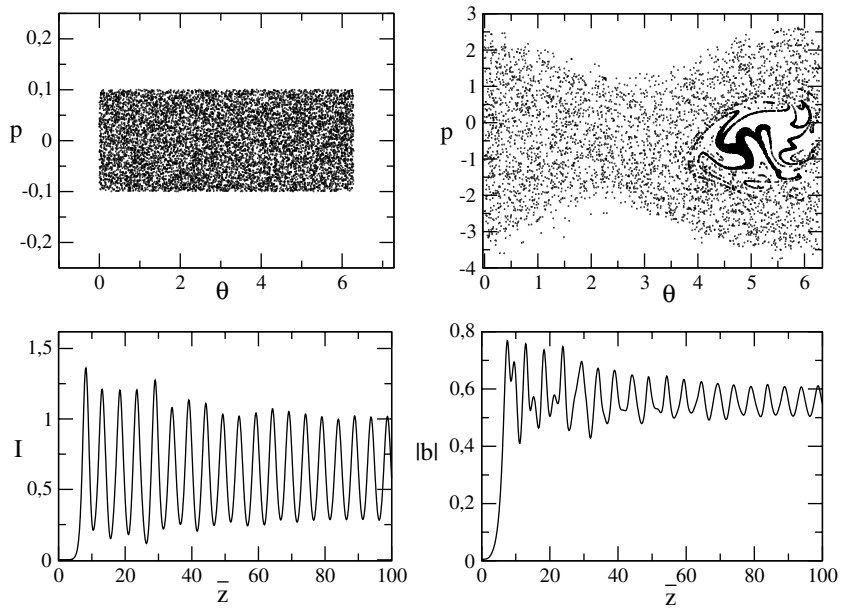

Fig. 3. Top-left panel: Initial phase-space portrait. A water-bag distribution, i.e. particles uniformly distributed within a closed support, is assumed. Top-right panel: Phase-space portrait at a later time. The presence of a dense core (*macroparticle*) is clearly displayed. Bottom-left panel: Evolution of the radiation intensity along the undulator $\bar{z}$. Bottom-right panel: Evolution of the bunching parameter along the undulator.

The latter conserves the energy and the momentum per particle.

In reference [4] it was shown that the average level of the intensity at saturation and the bunching parameters can be accurately predicted by performing a statistical mechanics treatment of the Vlasov equation, following the prescriptions of the pioneering work by Lynden-Bell [6]. This entails the possibility of identifying the QSS, where the discrete system gets trapped, with an equilibrium solution of the associated continuous set of equations.

On a more general level, QSS's manifest in many systems with long-range interactions and their characterization has originated an intense debate around the necessity of developing novel theoretical interpretative frameworks. In particular, the HMF model [2], a simplified one-dimensional Hamiltonian scheme for the coupled evolution of N rotators, has been widely employed to test the correctness of different predictions. Particularly interesting is the role played by the initial conditions in driving the system towards macroscopically different QSS. In this respect, it was argued in [13] that initially homogeneous (un-bunched) conditions constitute a rather special choice, against the broad class of spatially inhomogeneous (bunched) distributions. Several numerical works have then been devoted to investigating the dynamical anomalies that supposedly arise when starting with a bunched profile [14,15]. On a theoretical ground it should be mentioned that homogeneous distributions correspond to Vlasov stable equilibria, an argument invoked in [16] to stress their specificity. As opposite to this vision, a unifying theoretical scenario was proposed in [5] where the Lynden-Bell Vlasov based approach is successfully applied, irrespectively of the initial degree of particles bunching.

We will here further contribute to the debate by numerically monitoring the evolution of a FEL in CHG configuration, which, as discussed in the previous section, is characterized by a bunched beam at the entrance of the radiator. The outcome of the simulations will be compared to the Lynden-Bell prediction.

The basic idea underlying the Lynden-Bell approach [4,17] is to coarse-grain the microscopic single-particle distribution function $f(\theta, p, t)$, which is filamented by the dynamics. An entropy is then associated to the coarse-grained function $\bar{f}$ by counting the number of microscopic configurations giving rise to it.

Starting with an initial centered water-bag distribution, which corresponds to a rectangle uniformly occupied in the phase space (θ, p):

$$f(\theta, p, 0) = \begin{cases} f_0 = 1/\left(4\theta_0 p_0\right) \text{ if } -p_0 < p < p_0 \text{ and } -\theta_0 < \theta < \theta_0 \\ 0 \qquad\qquad\qquad\qquad \text{otherwise} \end{cases} \tag{10}$$

the entropy can be expressed as [6,17]:

$$s(\bar{f}) = -\int \left[\frac{\bar{f}}{f_0}\ln\frac{\bar{f}}{f_0} + \left(1-\frac{\bar{f}}{f_0}\right)\ln\left(1-\frac{\bar{f}}{f_0}\right)\right] \mathrm{d}\theta\, \mathrm{d}p. \tag{11}$$

The equilibrium is computed by maximizing this entropy, while imposing the conservation of the energy, momentum and number of particles.

Performing the analytical calculation one gets

$$\bar{f} = f_0 \frac{e^{-\beta(p^2/2+2A\sin\theta)-\eta p-\mu}}{1+e^{-\beta(p^2/2+2A\sin\theta)-\eta p-\mu}} \quad (12)$$

$$A = \sqrt{A_x^2 + A_y^2} = -\frac{\beta}{\eta}\int \sin(\theta)\bar{f}(\theta,p)\,\mathrm{d}\theta\,\mathrm{d}p, \quad (13)$$

where β/f_0, η/f_0 and μ/f_0 are Lagrange multipliers, which are determined by the conservation constraints. From (13) one gets the estimates of the equilibrium values for the intensity I and the bunching parameter b_n.

As previously mentioned, in reference [4] the predictions obtained from these calculations have been compared to the numerical results for homogeneous initial conditions [$\theta_0 = \pi$ in Eq. (10)]. The agreement found is remarkably good and provides an *a posteriori* validation for the choice of the Vlasov statistical mechanics to describe the emergence of the QSS. We shall report in the next sections about the extension to the inhomogeneous (water-bag) initial condition.

4 Comparison with numerical results

The electron-beam phase space distribution at the entrance of the radiator can be approximated by a water-bag distribution, similar to that specified by equation (10)[1]. In this case, the spatial and energy widths, here labelled ψ_0 and p_0 respectively, follow from equations (5) and (6). Labelling with b_0 the bunching at the radiator entrance:

$$|b_0| = \int\int f(\psi,p,0)\exp(i\psi)\mathrm{d}\psi\mathrm{d}p = \frac{\sin\psi_0}{\psi_0}, \quad (14)$$

where $\psi = n^*\theta$ is the phase label in the radiator (θ being the phase in the modulator and dispersive section), which is tuned at the harmonic λ/n^*. The momentum width of the water-bag distribution is in turn defined in terms of the initial beam parameters:

$$p_0 = \frac{\sigma_{\gamma,tot}}{\gamma\rho}. \quad (15)$$

The latter specifies the initial (conserved) energy per particle, h_0, according to the following relation

$$h_0 = \int \frac{p^2}{2} f(\psi,p,0)\,\mathrm{d}\psi\,\mathrm{d}p = \frac{p_0^2}{6}. \quad (16)$$

Numerical simulations are performed using the discrete system (1-3). In Figure 4 the average intensity at saturation is reported as function of $|b_0|$, for different values of the initial kinetic energy. Results are compared with the analytical estimate obtained above. Analogous plots for the average value of the bunching parameter at saturation are reported in Figure 5. A direct inspection of the figures confirms the adequacy of the proposed theoretical framework: predictions based on the Vlasov theory correlate well with numerical curves. Note that we are here considering the general case in which $|b_0|$ and p_0 are independent parameters. The optimized case in which $|b_0|$ and p_0 are linked together trough the relation ($\Delta\gamma = n\sigma_\gamma$) [see Eqs. (5), (6) and (15)] will be considered in the following.

The theory is sufficiently accurate for all the cases displayed in Figures 4 and 5, that is for any $|b_0|$ and for all the energies below a critical threshold $h_{0c} \simeq 0.315$, where the system experiences a dynamical transition.

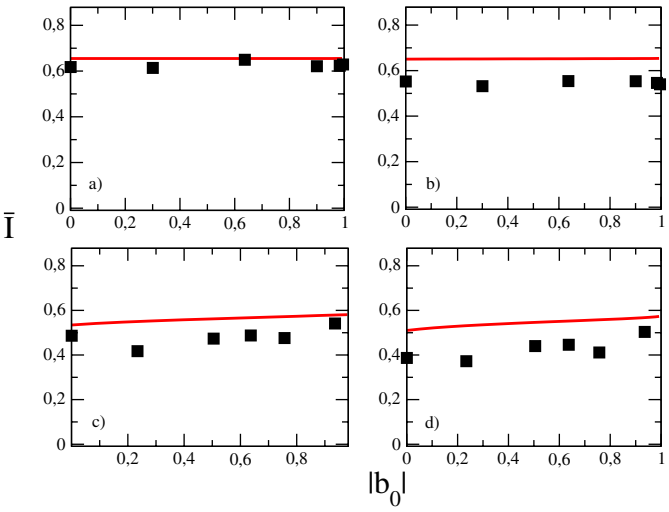

Fig. 4. Average intensity $\bar{I}$ at undulator exit as function of the initial bunching $|b_0|$ for different values of the initial average kinetic energy, respectively a) $h_0 = 0.01$ b) $h_0 = 0.16$ c) $h_0 = 0.21$ d) $h_0 = 0.315$. The continuous lines correspond to the theoretical predictions obtained in Section 3, while symbols represent numerical results obtained averaging intensity fluctuations in the saturated regime (see bottom-left panel of Fig. 3) over ten different realization of initial conditions giving the same ψ_0 and p_0.

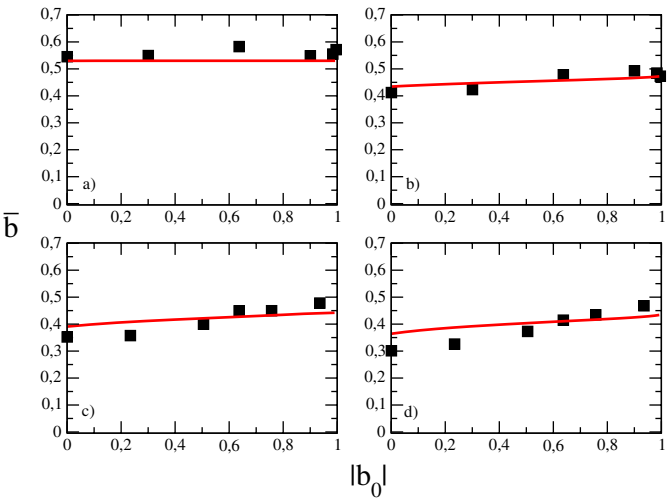

Fig. 5. Average values of the bunching parameter $|\bar{b}|$ at undulator exit as function of $|b_0|$. Same choice of parameters as Figure 4.

[1] The profile (10) represents a first order approximation of the electron distribution at the exit of the modulator when one neglects non-resonant particles and assume a uniform velocity distribution.

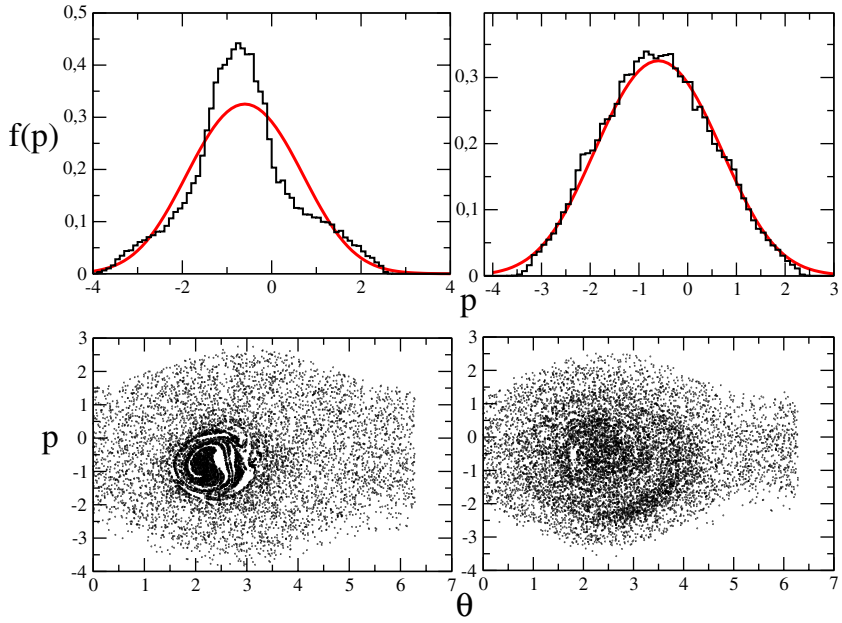

Fig. 6. Top: Velocity distributions of the particles for $h_0 = 0.1667$ and $\psi_0 = 0.785$ (left), 2.355 (right). The histograms are obtained from simulations with $\bar{z} = 100$ and result from an average over ten different realizations. The continuous lines represent the analytical result predicted by the first of equation (12). Bottom: Phase-space portraits corresponding to the two cases mentioned above. As before, $h_0 = 0.1667$ and $\psi_0 = 0.785$ (left), 2.355 (right).

In fact, as it is shown in [3], when $h_0 > h_{0c}$ the initial state is stable for $\psi_0 = \pi$, and the wave oscillates indefinitely without getting amplified. The system is hence prevented from eventually reaching the state predicted by the statistical mechanics and, as a consequence of this purely dynamical effect, the agreement is punctually lost. When increasing the value of the nominal energy h_0, the instability mechanism takes place only at larger value of b_0 and the agreement between theory and numerics progressively deteriorates (data not shown).

As a further check of the theory, we focused on the velocity distribution in the QSS. To this aim numerical results are compared to prediction (12). Two curves relative to $h_0 = 0.16$ and different values of the water-bag spatial support ψ_0 are displayed in Figure 6. For large ψ_0 (right plot in the figure), the agreement is excellent, and the solid line (theory) interpolates correctly the numerical histogram. To assess the goodness of fit both a Kolmogorov-Smirnov and a chi-square tests have been performed, under null hypothesis that the numerical sample comes from the Lynden-Bell distribution. The null hypothesis is rejected at level which is estimated below 1% for the Kolmogorov-Smirnov test and below 5% for the chi-square test, thus confirming the adequacy of the proposed theoretical approach. Conversely, when the initial distribution becomes narrower, which in turn corresponds to smaller values of ψ_0 (i.e., to larger bunching), the discrepancy between theory and numerics is enhanced. The source of this disagreement can be identified by looking at the evolution of the electron-beam phase space: when starting with a relatively large bunching parameter, the particle distribution gets more filamented during the initial violent relaxation and the cluster which asymptotically persists in the saturated regime tends to be more localized (see Fig. 6). This dense core of particles results in the central peak which appears in the velocity profile for smaller ψ_0, as shown in Figure 6. The presence of such localized structure contradicts the mixing hypothesis assumed within the Lynden-Bell scenario. However, the predictions for the quantities of interest, namely the average intensity and the bunching parameter, are satisfactory. Indeed, the presence of the macroparticle mainly influences the oscillations of such quantities, their mean value being correctly reproduced by the theory.

The theoretical analysis developed in this paper constitutes a novel strategy to predict the intensity at saturation for a CHG setting, provided the value of the incoherent energy spread is assigned and without resorting to direct numerical investigations. In fact, the knowledge of σ_γ enables to directly calculate $\Delta\gamma$ ($= n\sigma_\gamma$) and $\sigma_{\gamma,tot}$ by means of equation (6), and consequently estimate both $|b_0|$ and p_0, based on equations (14–15). The spatial width, ψ_0, of the initial water-bag distribution is finally derived by inverting relation $|b_0| = \sin(\psi_0)/\psi_0$. Once the values of ψ_0 and p_0 are specified according to the above strategy, the theory of the violent relaxation outlined above allows to quantitatively predict the saturated state of the system.

To validate the proposed theoretical framework, we have considered the case of the CHG project FERMI@Elettra [18] and focused in particular on the experimental setting relative to the output wavelength 40 nm. In this case, $n = 6$ (i.e., the initial seed wavelength is 240 nm), $\gamma = 2310$, $\sigma_\gamma = 200$ KeV and $\rho \simeq 2.8 \times 10^{-3}$. Direct numerical simulations are performed using GENESIS [19], a three dimensional code that explicitly accounts for the coupling between the transverse and longitudinal

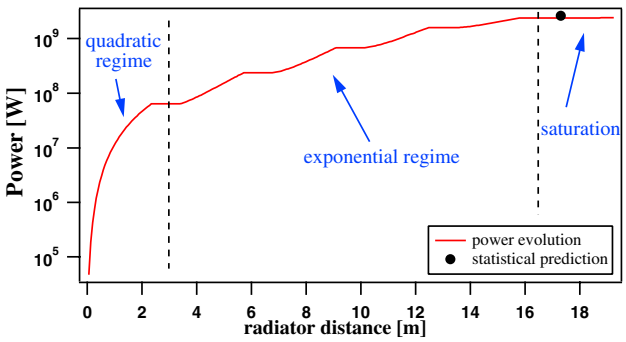

Fig. 7. Power growth (in logarithmic scale) along the radiator distance obtained using the 3D numerical code GENESIS. The full circle represents the statistical prediction. In the numerical curve one can distinguish a first quadratic growth (up to about 3 m), followed by an exponential amplification. Saturation occurs at about 16.5 m. The saturation plateau is at 2.4 GW, while the statistical calculation gives 2.6 GW. The undulator is subdivided in six segments of about 2.3 m separated by drift sections of 1 m. In the drifts the electron beam is refocused by means of magnetic quadrupoles and the light is not amplified.

dimensions. Assuming a radiator length of 19 m, a horizontal and vertical (normalized) beam emittance of 1.5 μ m and an optical waist of $w \simeq 350$ μm, simulations give an output power of about 3 GW. The power evolution along the radiator distance is shown in Figure 7, where the statistical prediction is also displayed. The numerical simulation correlates extremely well with the theory developed above, the disagreement being less than 10%. Such a result validates the choice of a water bag to approximate the more realistic (i.e., bell-shaped) electron-beam distribution utilized by GENESIS at the undulator entrance.

5 Conclusions and perspectives

Results reported in this paper are of twofold interest. On one hand, they provide a significant contribution to the intense debate about the appropriate statistics to be adopted for the description of long-range interacting systems. In this respect, we demonstrated that a maximum entropy principle inspired to Lynden-Bell's theory of "violent relaxation" for the Vlasov equation allows to satisfactorily predict the quasi-stationary (saturated) state of a single-pass FEL operated in CHG regime. These findings confirm what has been recently demonstrated in [4] and [5] in the context of the SASE FEL and of the HMF model, respectively. Despite this success, we are aware that Lynden-Bell's method is not expected to be always very precise, mainly due to incomplete relaxation of the Vlasov equation. Collective effects may develop giving rise to massive agglomeration, enhanced by local dynamical traps. These mechanisms prevent perfect mixing to occur and weaken the ergodic hypothesis on which the "violent relaxation" theory is built. A more detailed analysis of such phenomena will be the object of our future investigation. On the other hand, the method we have developed provides a powerful analytical tool that can be exploited for the design of a single-pass FEL. Such a method is presently limited to situations in which one can neglect transverse effects. This happens when the electron-beam geometrical emittance is smaller than the radiation wavelength, the beam relative energy spread is smaller than the Pierce parameter ρ and the Rayleigh length of emitted radiation is much longer than the radiator length. This is for instance the case of the whole spectral range that will be covered by the FERMI@Elettra FEL (100–10 nm).

We thank J. Barré, T. Dauxois and S. Ruffo for fruitful discussions.

References

1. *Dynamics and Thermodynamics of Systems with Long Range Interactions*, edited by T. Dauxois, S. Ruffo, E. Arimondo, M. Wilkens, Lecture Notes in Physics, Vol. 602 (Springer, 2002)
2. M. Antoni, A. Ruffo, Clustering and relaxation in long range Hamiltonian dynamics, Phys. Rev. E **52**, 2361 (1995)
3. R. Bonifacio et al., Opt. Comm. **50**, 373 (1984)
4. J. Barré et al., Phys. Rev. E **69**, 045501 (2004)
5. A. Antoniazzi, D. Fanelli, J. Barré, P.H. Chavanis, T. Dauxois, S. Ruffo, Phys. Rev. E **75**, 011112 (2007)
6. D. Lynden-Bell, Mon. Not. R. Astron. Soc. **136**, 101 (1967)
7. S Milton et al., Science **292**, 2037 (2003)
8. L.H. Yu et al., Science **289**, 932 (2000)
9. L.H. Yu, Phys. Rev. A **44**, 5178 (1991)
10. A. Antoniazzi, G. De Ninno, A. Guarino, D. Fanelli, S. Ruffo, J. Phys. **7**, 143 (2005)
11. A. Antoniazzi, Y. Elskens, D. Fanelli, S. Ruffo Eur. Phys. J. B **50**, 603 (2006)
12. M.C. Firpo, Y. Elskens, J. Stat. Phys. **93**, 192 (1998)
13. A. Pluchino, V. Latora, A. Rapisarda, Physica A **338**, 60 (2004)
14. A. Pluchino, V. Latora, A. Rapisarda, Phys. Rev. E **69**, 056113 (2004)
15. V. Latora, A. Rapisarda, C. Tsallis, Phys. Rev. E **64**, 056134 (2001)
16. A. Rapisarda et al. Europhysics News **36**, 2002 (2005)
17. P.H. Chavanis, J. Sommeria, R. Robert, Astrophys. J. **471**, 385 (1996)
18. See `http://www.elettra.trieste.it/FERMI/`
19. `http://pbpl.physics.ucla.edu/reiche/`